APJAI
Asian Pacific Journal of
Allergy and Immunology

ORIGINAL ARTICLE

Deciphering critical amino acid residues to modify and enhance the binding affinity of ankyrin scaffold specific to capsid protein of human immunodeficiency virus type 1

Somphot Saoin,[1,2] Tanchanok Wisitponchai,[1,2] Kannaporn Intachai,[1,2] Koollawat Chupradit,[1,2] Sutpirat Moonmuang,[1,2] Sawitree Nangola,[3] Kuntida Kitidee,[4] Kanda Fanhchaksai,[1,2] Vannajan Sanghiran Lee,[5,6] Saw-See Hong,[7,8] Pierre Boulanger,[7,8] Phimonphan Chuankhayan,[9] Chun-Jung Chen,[9,10,11] Chatchai Tayapiwatana[1,2]

Abstract

Background: Ank^{GAG}1D4 is an artificial ankyrin repeat protein which recognizes the capsid protein (CA) of the human immunodeficiency virus type 1 (HIV-1) and exhibits the intracellular antiviral activity on the viral assembly process. Improving the binding affinity of Ank^{GAG}1D4 would potentially enhance the Ank^{GAG}1D4-mediated antiviral activity.

Objective: To augment the affinity of Ank^{GAG}1D4 scaffold towards its CA target, through computational predictions and experimental designs.

Method: Three dimensional structure of the binary complex formed by Ank^{GAG}1D4 docked to the CA was used as a model for van der Waals (vdW) binding energy calculation. The results generated a simple guideline to select the amino acids for modifications. Following the predictions, modified Ank^{GAG}1D4 proteins were produced and further evaluated for their CA-binding activity, using ELISA-modified method and bio-layer interferometry (BLI).

Results: Tyrosine at position 56 (Y56) in Ank^{GAG}1D4 was experimentally identified as the most critical residue for CA binding. Rational substitutions of this residue diminished the binding affinity. However, vdW calculation preconized to substitute serine for tyrosine at position 45. Remarkably, the affinity for the viral CA was significantly enhanced in Ank^{GAG}1D4-S45Y mutant, with no alteration of the target specificity.

Conclusions: The S-to-Y mutation at position 45, based on the prediction of interacting amino acids and on vdW binding energy calculation, resulted in a significant enhancement of the affinity of Ank^{GAG}1D4 ankyrin for its CA target. Ank^{GAG}1D4-S45Y mutant represented the starting point for further construction of variants with even higher affinity towards the viral CA, and higher therapeutic potential in the future.

Keywords: ankyrins; Ank^{GAG}1D4; HIV-1 assembly; capsid; computer-aided molecular design

From:
[1] Division of Clinical Immunology, Department of Medical Technology, Faculty of Associated Medical Sciences, Chiang Mai University, Chiang Mai, Thailand
[2] Center of Biomolecular Therapy and Diagnostic, Faculty of Associated Medical Sciences, Chiang Mai University, Chiang Mai, Thailand
[3] Division of Clinical Immunology and Transfusion Sciences, School of Allied Health Sciences, University of Phayao, Phayao, Thailand
[4] Center for Research and Innovation, Faculty of Medical Technology, Mahidol University, Bangkok, Thailand
[5] Thailand Center of Excellence in Physics, Commission on Higher Education, Bangkok, Thailand
[6] Department of Chemistry, Faculty of Science, University of Malaya, Kuala Lumpur, Malaysia
[7] Viral Infections and Comparative Pathology, UMR-754 UCBL-INRA-EPHE, Université Lyon 1, Lyon Cedex 07, France
[8] Institut National de la Santé et de la Recherche Médicale, Paris, France
[9] Life Science Group, Scientific Research Division, National Synchrotron Radiation Research Center, Hsinchu, Taiwan
[10] Department of Physics, National Tsing Hua University, Hsinchu, Taiwan
[11] Institute of Biotechnology and Center for Bioscience and Biotechnology, National Cheng Kung University, Tainan, Taiwan

Corresponding author:
Chatchai Tayapiwatana
Division of Clinical Immunology,
Department of Medical Technology, Faculty of Associated Medical Sciences, Chiang Mai University, Chiang Mai, Thailand 50200
E-mail: asimi002@hotmail.com

Introduction

Antibodies have been implemented for many medical applications and represented the largest class of therapeutic proteins in clinical development.[1,2] However, therapeutic antibodies have several limitations, such as their relatively high production cost, inefficient penetration and insufficient retention in targeted tissues.[3,4] In addition, the major inconvenience is the requirement of disulfide bond formation to stabilize their structure and biological activity, a biochemical process which cannot occur in the reducing intracellular milieu. To address these limitations, non-immunoglobulin scaffolds have been proposed as alternatives to antibodies.[5,6] These protein scaffolds were selected according to the following criteria: their high degree of solubility and stability, independence of disulfide bonds and/or glycosylation sites, their low cost of production, and their high affinity for their targets.[5]

Ankyrins, and their artificial derivatives designed ankyrin repeat proteins (DARPins), are a novel class of protein binders designed for the recognition of a variety of molecular targets with high specificity and affinity. They are biologically active in various environments, including the extracellular milieu and intracellular compartments.[7-10] Applications of artificial ankyrins to antiviral treatments are a new challenge for the future therapeutics, and recently, antiretroviral ankyrins have been designed to inhibit HIV-1 replication. This is the case for a CD4-specific DARPin, which competes with the HIV-1 envelope gp120 for CD4-receptor binding, and blocks the cell entry of divergent strains of HIV-1.[11] Likewise, a gp120 -reactive DARPin interacting with the V3 loop of gp120 acts as an efficient HIV-1 entry inhibitor.[12]

Ank^{GAG}1D4 is a trimodular repeat protein which was selected from a phage-displayed ankyrin library for its binding to the HIV-1 capsid (CA).[13] Ank^{GAG}1D4 has been shown to possess a significant antiviral effect against HIV-1 replication.[13,14] HIV-1-infected SupT1 cells stably expressing Ank^{GAG}1D4 showed a significant reduction of the viral progeny yield, compared to control SupT1 cells.[13] Likewise, the N-myristoylated version of Ank^{GAG}1D4 was found to negatively interfere with HIV-1 replication in primary human CD4+ T-cells.[14] Ank^{GAG}1D4 showed a relatively high performance in terms of inhibition of viral particle assembly, but its efficacy, in terms of protection from HIV-1 infection, was not maximal, especially at late phase postinfection.

Increasing the affinity of Ank^{GAG}1D4 towards its viral target seemed therefore a well designated strategy to enhance the Ank^{GAG}1D4-mediated antiviral activity to obtain a complete HIV-1 inhibition. Several strategies are available to achieve this goal. In the present study, we used a relatively simple but rational approach through computational design, as an alternative to the time-consuming method of combinatorial design or directed evolution of ankyrin genes, using error-prone PCR in combination with *in vitro* selection of modified ankyrins by ribosome-display or phage-display.[9,11]

The goal of this study was to enhance binding affinity of Ank^{GAG}1D4 towards its viral target, through manipulation of selected amino acids belonging to the binding site or located in its close vicinity. Our choice of amino acid residues to modify in Ank^{GAG}1D4 was guided by the position and nature of the major determinants of the CA binding, deduced from crystal structure and computational analysis. Calculation of the van der Waals (vdW) binding forces guided us in our choice of the amino acid positions to target in the ankyrin sequence. The biological effects of these mutations on the affinity of Ank^{GAG}1D4 towards the CA were evaluated using ELISA-derived immunological tests and bio-layer interferometry. This computationally guided molecular design, which involved molecular structures and vdW binding energy of interacting molecules, provided a rational method for the modification of binding parameters, and represented a gain in time compared to other strategies.

Methods

Structure-guided enhancement of the affinity of Ank^{GAG}1D4 towards the viral CA

Ank^{GAG}1D4 residues, S45, Y56, R89, K122 and K123 were identified as key residues in the CA-binding. All key residues were substituted to the 20 natural amino acids (with the exception of S, Y, R or K, respectively for each case). Y56 was the major key residue of the CA-binding, while the other residues were secondary players in this interaction. These residues were categorized by the frequency of the interaction pairs as described in our previous paper.[15] In the CA/Ank^{GAG}1D4 complexes, the CA structure was fixed, and the Ank^{GAG}1D4 mutants were minimized by the algorithms of Steepest Descent and followed by Conjugate Gradient, based on CHARMM19 force field. The vdW values at positions 45, 56, 89, 122 and 123 in Ank^{GAG}1D4-CA mutants interacting with CA in our simulated models were compared to the residues found at the corresponding positions in parental Ank^{GAG}1D4.

Site-directed mutagenesis of Ank^{GAG}1D4

Plasmid pQE30 encoding the full-length Ank^{GAG}1D4 was used for the amplification of the first ankyrin module (module#1) which contained the S45 or Y56 residues in standard PCR method. PCR was carried out using KOD Hot Start DNA polymerase (Novagen, Madison, WI). After purification, the amplified fragment was ligated into the pTZ57R/T acceptor vector, using the InsTAclone PCR Cloning Kit (Thermo Scientific, Rockford, IL). The ligation product was then introduced into the *E.coli* XL1-blue strain. The correctness of the clones was verified by standard sequencing method. The pTZ57R/T plasmid carrying the Ank^{GAG}1D4 module#1 was purified, and used as template for site-directed mutagenesis of S45 or Y56 residues by using the Quick change® lightening site-directed mutagenesis kit (Stratagene, La Jolla, CA).

Construction of expression vector encoding Ank^{GAG}1D4 mutants

The DNA fragments encoding module#1 mutants were amplified from the corresponding pTZ57R/T plasmids as above. The DNA fragment encoding the second module linked to the third module of Ank^{GAG}1D4 (module#2+module#3) were amplified from the pQE30-Ank^{GAG}1D4 plasmid. The DNA fragments encoding the module#1 mutants and the DNA fragment encoding module#2+module#3 were then assembled using the Gibson Assembly® Master Mix (New England Biolabs, Ipswich, MA). Next, the trimodular sequences carrying the mutations in module#1 were amplified using the KOD Hot Start DNA polymerase (Novagen, Madison, WI) subsequently

treated with *Not*I and *Hind*III. The amplified fragments were ligated with the pQE30 plasmid which had been cleaved with the same enzymes. The ligated products were used to transform XL1-blue competent cells. The new constructs of pQE30-Ank^{GAG}1D4 mutants were transferred to *E. coli* strain M15[pREP4] for recombinant protein expression. The recombinant Ank^{GAG}1D4 mutant proteins were produced and purified as described in detail elsewhere.[13,15]

Production of recombinant CA protein from bacterial cells

The recombinant CA protein was expressed following the protocol previously described.[15] The protein was purified by affinity chromatography on HisTrap column, using ÄKTA Prime™ plus (GE Healthcare, Piscataway, NJ). Protein concentration was measured using the Bradford protein assay kit (Pierce/Thermo Scientific, Rockford, IL) and analyzed by western blotting. In addition, the biotinylated CA was prepared by using EZ-Link™ Sulfo-NHS-LC-Biotinylation kit (Pierce/Thermo Scientific, Rockford, IL) according to the procedure recommended by the manufacturer.

Evaluation of the CA-binding activity of Ank^{GAG}1D4 and Ank^{GAG}1D4 mutants

The binding of Ank^{GAG}1D4 and Ank^{GAG}1D4 mutants to the CA protein was evaluated using AMELIA, a modification of the conventional ELISA, consisting of ankyrin-mediated capture of the target protein, followed by enzyme-linked immunoassay.[15] The microtiter plate was directly coated with recombinant Ank^{GAG}1D4 or Ank^{GAG}1D4 mutants at a final concentration of 5 µg/mL overnight at 4°C. Purified CA protein, diluted in PBS-2% bovine serum albumin (BSA), was added, and incubated at RT for 1h. After incubation, the excess amount of CA was removed using a conventional washing buffer (0.05% Tween-20 in PBS) or a high stringency washing buffer (1% Triton X100 (v/v) and 550 mM NaCl prepared in PBS (136.9 mM NaCl, 2.7 mM KCl, 8.1 mM Na_2HPO_4 and 1.5 mM KH_2PO_4), pH7.4).[16] The level of Ank^{GAG}1D4-mediated capture of the target CA protein was detected using the mouse monoclonal antibody against CA protein (M88), followed by HRP-conjugated goat anti-mouse immunoglobulin.

Binding kinetic analysis by bio-layer interferometry (BLI)

The binding kinetics of the Ank^{GAG}1D4 mutants with recombinant CA were measured using BLI performed with the BLItz™ system (ForteBio, Menlo Park, CA). All interaction analyses were conducted in sample diluent (bovine serum albumin (w/v, 2%) and tween-20 detergent (v/v, 0.05%) in PBS). Streptavidin (SA) biosensors were pre-wetted for 15 min in buffer immediately before use. The microplates used in the ForteBio system were filled with sample diluent for 250 µl/well. Biotinylated CA protein at 100 µg/mL was immobilized to Streptavidin (SA) biosensors for 2 min. Next, saturated biosensors were washed in sample diluent for 30 sec and transferred to the tubes containing 10 µg/mL Ank^{GAG}1D4 parental or mutants in diluent buffer. The association and dissociation values of Ank^{GAG}1D4 parental and mutants were measured for each step of 1.30 min. Kinetic parameters (k_{on} and k_{off}) and the equilibrium dissociation constant (K_D) were calculated from a non-linear local fit of the data between Ank^{GAG}1D4 and CA proteins, using the BLItz Pro 1.1 software. To test the specificity, biotinylated interferon-γ (IFN-γ) which was also immobilized to SA biosensor, was used as irrelevant protein target served as negative control.

Determination of the CA ankyrinotope binding of Ank^{GAG}-1D4-S45Y

AMELIA was applied to competitive system for analyzing the binding site on CA of Ank^{GAG}1D4-S45Y mutant. Each of ankyrin including parental Ank^{GAG}1D4, Ank^{GAG}1D4-S45Y and Ank^{GAG}1D4-Y56A (final concentration of 10 µg/mL) was coated overnight at 4°C. Biotinylated CA protein (final concentration of 2.8 µg/mL) was added and incubated at RT for 1 h. After washing with high stringency buffer, the competitors in solution comprising recombinant Ank^{GAG}1D4, Ank^{GAG}1D4-S45Y, Ank^{GAG}1D4-Y56A and interferon-γ (IFN-γ), irrelevant protein (R&D Systems, Minneapolis, MN), at final concentration of 10 µg/mL were individually added to each well. The wells were washed and followed by addition the HRP -conjugated anti-biotin.

Results

Choice of amino acid residue(s) as target(s) for editing

Tyrosine at position 56 (Y56) in Ank^{GAG}1D4 was identified by molecular docking analysis as the key residue contributing the most to the binding of Ank^{GAG}1D4 to its viral partner.[15] The first step of our study was to experimentally verify that Y56 really played a crucial role in this interaction. If confirmed, this would designate Y56 as a candidate residue for the modulation of the binding affinity of Ank^{GAG}1D4 towards the CA. To this aim, we generated the substitution mutant Ank^{GAG}1D4-Y56A by site-directed mutagenesis of tyrosine at position 56 into alanine. The binding reactivity of Ank^{GAG}1D4 -Y56A recombinant protein to CA was evaluated by AMELIA, an ELISA-modified method based on the ankyrin-mediated capture of the target protein, followed by enzyme-linked immunoassay.[15] The parental ankyrin Ank^{GAG}1D4 showed a high CA-binding activity towards the viral CA protein, and the interaction observed between the two partners occurred in a CA concentration-dependent manner. In contrast, no CA -binding activity was detectable for the Ank^{GAG}1D4-Y56A mutant, at all CA concentrations tested (**Figure 1A**). This confirmed experimentally our previous prediction that Y56 was a first-rank key residue for the binding of HIV-1 CA,[15] and designated this residue as the best candidate for modification.

To further investigate on the role of residue Y56 in the binding of Ank^{GAG}1D4 to the CA, Ank^{GAG}1D4-Y56A mutant protein was purified to homogeneity and crystallized, and a structural analysis Ank^{GAG}1D4-Y56A crystal was performed. The structure of Ank^{GAG}1D4-Y56A crystal was determined at 1.9 Å resolution (accession codes 4ZFH). All X-ray crystallographic data and refinement statistics are summarized in **Table 1**. The result demonstrated that the overall structure of Ank^{GAG}1D4-Y56A was similar to that of Ank^{GAG}1D4 parental, as shown by the superimposition of the two crystal structures. The root mean square deviation (RMSD) of the Cα backbone between Ank^{GAG}1D4-Y56A mutant and Ank^{GAG}1D4

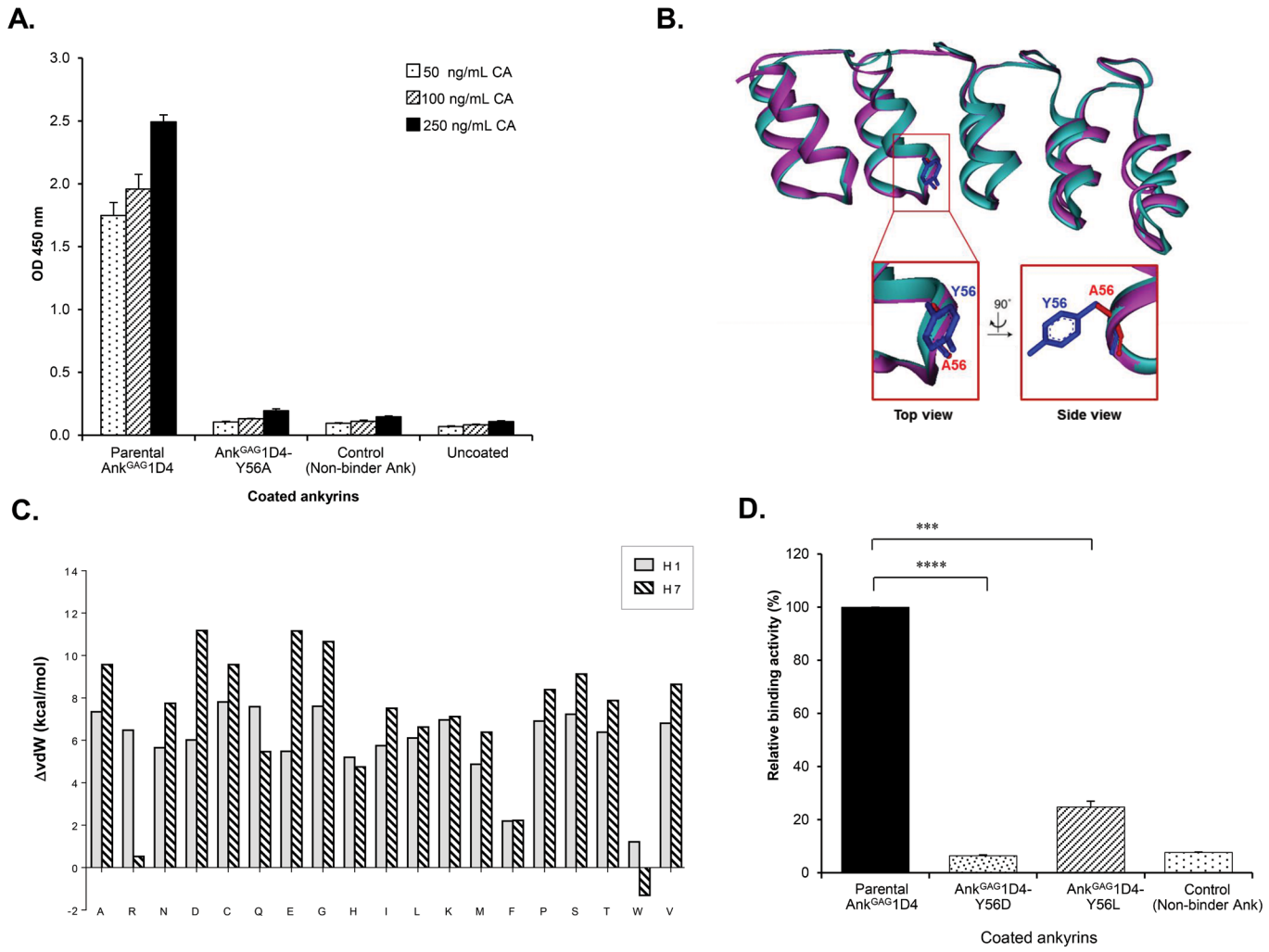

Figure 1. Effect of tyrosine substitution at position 56 on the interaction of Ank^{GAG}1D4 with the CA protein of HIV-1. (A) The CA-binding activity of the Ank^{GAG}1D4-Y56A mutant was compared with that of parental Ank^{GAG}1D4, using AMELIA. Samples of ankyrin proteins, parental Ank^{GAG}1D4, Ank^{GAG}1D4-Y56A mutant, and a non-binder ankyrin as negative control, were used at a concentration of 5 μg/mL, and coated on ELISA plate. After rinsing, CA protein was added to each well at increasing concentrations. Ankyrin-bound CA was detected using anti-CA mouse monoclonal antibody, followed by HRP-conjugated goat anti-mouse immunoglobulin. Negative control consisted of an irrelevant ankyrin protein which did not bind to CA. Results presented are from triplicate experiments (mean ± SD). (B) Superimposition of the crystal structures of parental Ank^{GAG}1D4 (cyan) and Ank^{GAG}1D4-Y56A mutant (purple), in ribbon-style representation. The square boxes show close-up views of Y56 (blue) and A56 (red) residues in the superimposed crystal structures. (C) Screening of amino acid substituents at position 56 in the Ank^{GAG}1D4 binding surface and assessment of their CA-binding activity. The differences in the vdW energy between mutant residues and Y56 were calculated for the H1-mediated (filled bars) and H7-mediated (hatched bar) modes of CA-binding, using the CHARMM19 force field program and the Momany-Rone algorithm. (D) CA-binding activity of selected Ank^{GAG}1D4 substitution mutants at position 56, analyzed by AMELIA. The binding activity was measured at OD_{450}, and the signal obtained with parental Ank^{GAG}1D4 and CA protein was attributed the 100% value. The relative binding activity was calculated using the following formula: $[OD_{mutant}/OD_{parental}]\times100$. Data presented are from triplicate experiments (mean ± SD), analyzed using one-way ANOVA. ***$P < 0.001$ and ****$P < 0.0001$.

parental was ~ 0.49 Å (**Figure 1B**), and no significant structural alteration resulted from the substitution of tyrosine by alanine. This strongly suggested that the loss of CA-binding activity in Ank^{GAG}1D4-Y56A mutant was due to the loss of the tyrosine ring at position 56, and not to the overall conformation of the ankyrin mutant molecule.

Substitutions of the first-rank key residue at position 56: predictions and experimental results

The computational prediction using 3D docking structures and calculation of vdW binding forces suggested that none of the 19 natural amino acids which would substitute for Y56 would confer any significant affinity improvement to the Ank^{GAG}1D4 mutants (**Figure 1C**). This was experimentally confirmed by introducing some representatives of these substitutions into the recombinant ankyrin protein, viz. Y56D and Y56L. These two ankyrin mutants had lost their capacity to bind to the CA (**Figure 1D**). The results demonstrated that Y56 was the most

Table 1. Statistics of X-ray diffraction data and structurerefinement of Ank^{GAG}1D4-Y56A mutant.[(a)]

Data collection	
Space group	C2
Cell dimension (Å)	a = 104.84, b = 28.64, c = 53.54 β = 106.39°
Resolution range (Å)	50–1.89
Observed reflections Total Unique	 58,430 11,686
Completeness (%)	98.2 (96.2)
Redundancy	5.0 (4.8)
R_{sym} (%)	5.6 (22.9)

Refinement	
Resolution range (Å)	50–1.89
R_{work}/R_{free} (%)	21.1/27.6
Average B-factor (Å^2)	20.9
RMS deviation from ideal geometry Bond lengths (Å) Bond angle (°)	 0.016 1.87

(a) Values in parenthesis in the right column correspond to the highest-resolution shell (1.94–1.89 Å).

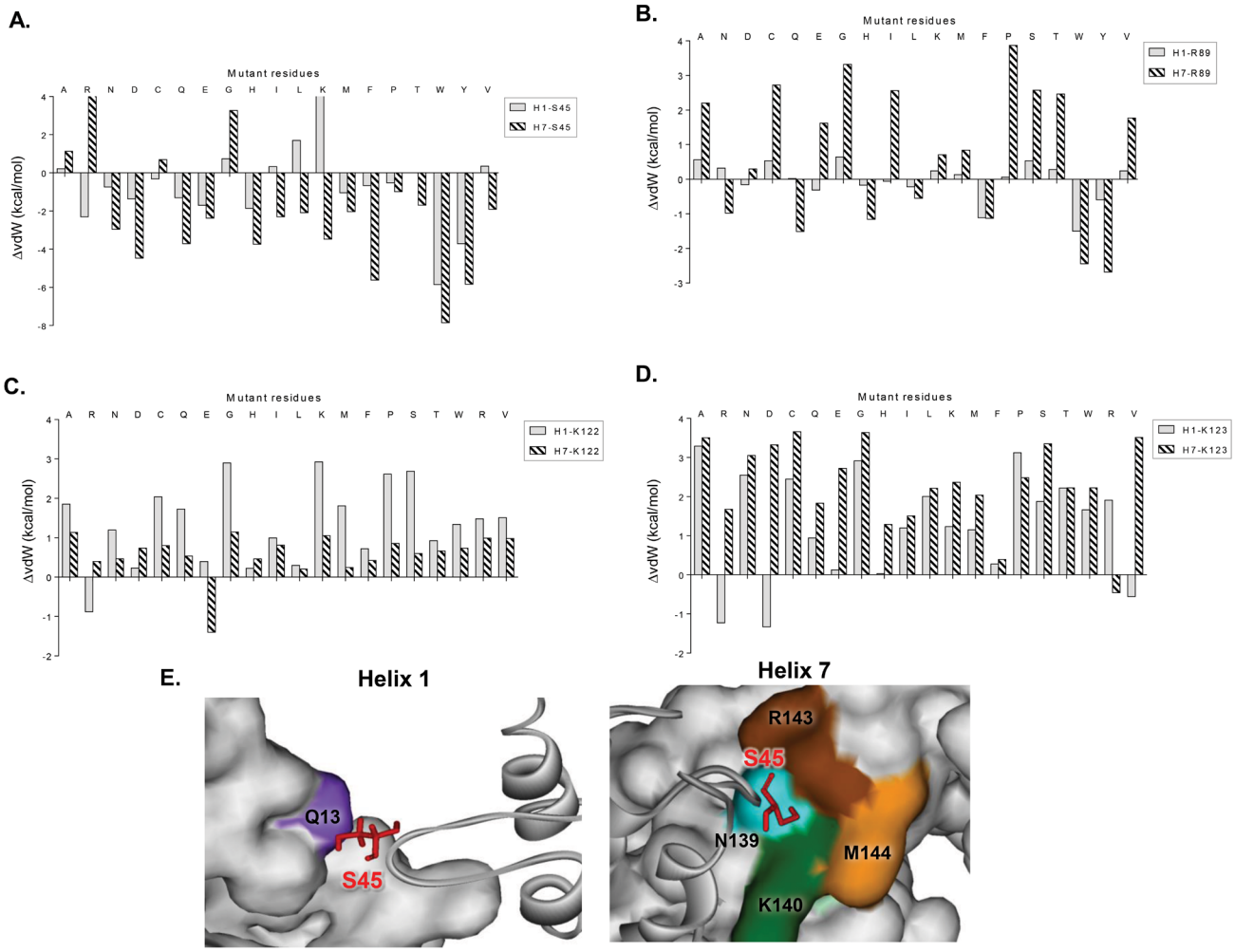

Figure 2. Screening of amino acid substituents at position 45, 89, 122 and 123 in Ank^{GAG}1D4. (A-D) Bar-graph of the ΔvdW values between mutant residues and serine 45 (A), arginine 89 (B), lysine 122 (C) and lysine 123 (D). The binding energy optimization was performed by screening 19 natural amino acid residues at these four positions in Ank^{GAG}1D4, when bound to the CA protein *via* the H1 or H7 alpha-helix of the CA N-terminal domain. The differences in the vdW energy between each one of the 19 mutant residues and the indicated parental residue were calculated for the H1-mediated (filled bars) and H7-mediated (hatched bars) modes of CA-binding, using the CHARMM19 force field program and the Momany-Rone algorithm. (E) Pocket analysis within 5 Å-distance of serine at position 45 (S45) in Ank^{GAG}1D4 binding to CA target. Red (in stick style representation) on ribbon style of Ank^{GAG}1D4 belongs to S45 residues. The amino acids surrounding S45 residue on CA protein representing in surface style are shown by different colors in H1-mediated (left panel) and H7-mediated (right panel) modes of CA-binding.

critical residue in the interaction with CA partner and could not be substituted for any other amino acid without profoundly altering the affinity.

Substitutions of second-rank key residues

The results obtained with mutants at position 56 led us to consider substitutions of residues S45, R89, K122 and K123, which were identified as second-rank determinants of the interaction of Ank^{GAG}1D4 with CA, compared to Y56.[15] As for the amino acid screening at position 56, these four residues were substituted by a panel of 19 natural amino acids, and the corresponding vdW energy calculated and compared to that of the parental Ank^{GAG}1D4. Mutant residues with ΔvdW values lower than -2 kcal/mol were considered as good candidates for conferring to Ank^{GAG}1D4 mutants a higher affinity to the CA (**Figure 2A-2D**). As previously, the selected mutations were introduced in the Ank^{GAG}1D4 gene, and the recombinant protein mutants analyzed in vitro for CA binding activity. In the case of K122 and K123, there was no substituent providing a ΔvdW lower than -2 kcal/mol (**Figure 2C and 2D**). Likewise, R89 substitution by tryptophan or tyrosine residue resulted in ΔvdW values of -2.68 and -2.43 kcal/mol, respectively. These two values were only slightly lower than the threshold value of -2 kcal/mol, and were only obtained in the H7-mediated mode of CA-binding (**Figure 2B**).

In the case of S45 however, 11 amino acid substituents out of 19 showed a ΔvdW value significantly lower than -2 kcal/mol (**Figure 2A**). This implied that position 45 represented a privileged target for the modulation of the binding affinity of Ank^{GAG}1D4 towards the CA. In both H1- and H7-mediated modes of CA binding, tryptophan and tyrosine residues were the two residues at position 45 which showed the lowest ΔvdW values: -5.85 and -3.72 kcal/mol, respectively, in the H1-mediated mode of CA binding; -7.85 and -5.84 kcal/mol, respectively, in the H7-mediated mode (**Figure 2A**).

Position 45 corresponded to an interfacial residue located on an external loop of the Ank^{GAG}1D4, and of ankyrin molecules in general. Sequence comparison showed that the residues at position 45 in 96% of 500 ankyrin sequences available in Uniref90 database analyzed by ConSurf server[17,18] were more hydrophilic than hydrophobic[19] (data not shown). Tyrosine is also less hydrophobic than tryptophan, therefore S45Y was selected as mutant, and the recombinant protein mutant Ank^{GAG}1D4-S45Y was generated as described above. As a further support to the vdW calculation-based prediction of S45 mutants, pocket analysis at position 45 showed that protein interaction within the 5Å-distance with ankyrin involved Q13 residue in the H1-mediated CA-ankyrin complex, and N139, K140, R143, M144 residues in the H7-mediated CA-ankyrin complex. Both pockets contributed to the binding through vdW bonds rather than through electrostatic interactions (**Figure 2E**).

Evaluation the effect of S-to-Y replacement at position 45 of Ank^{GAG}1D4 mutant on the CA-binding activity

To verify these predictions, the binding affinity of the Ank^{GAG}1D4-S45Y mutant towards the CA was evaluated by AMELIA in which a high-stringency washing buffer was

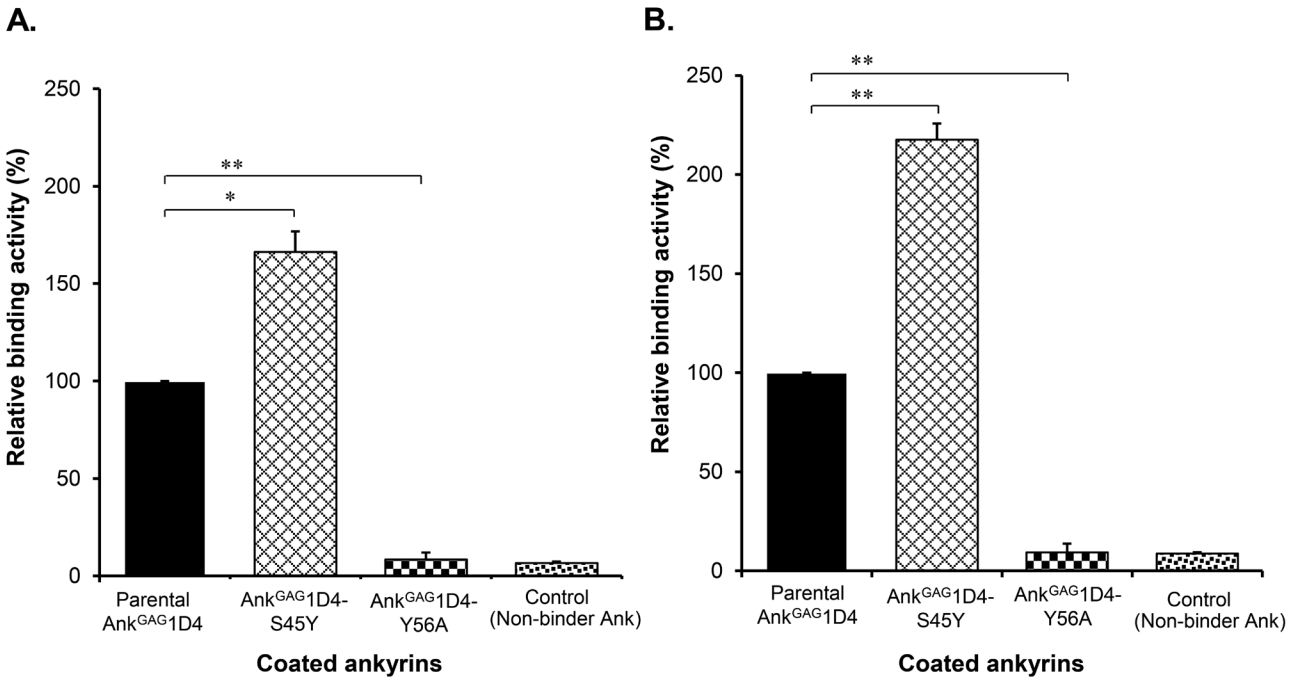

Figure 3. Effect of S-to-Y substitution at position 45 on the CA-binding activity of Ank^{GAG}1D4-S45Y mutant. The binding activity of Ank^{GAG}1D4 substitution mutants at position 45 was assessed by AMELIA using a conventional washing buffer (A), or a high stringency washing buffer (B). The binding activity was measured at OD_{450}, and the signal obtained with parental Ank^{GAG}1D4 and CA protein was attributed the 100% value. The relative binding activity was calculated using the following formula: [OD_{mutant}/$OD_{parental}$]×100. Results presented are from triplicate experiments (mean ± SD), analyzed using one-way ANOVA. *P < 0.05, **P < 0.01.

introduced in the washing step, in order to eliminate nonspecific binding, and to discriminate between high and low affinity binder.[16] The results showed that the binding activity of Ank^{GAG}1D4-S45Y was significantly higher than parental Ank^{GAG}1D4, 60% under conventional conditions and 110 % under high stringency conditions (**Figure 3**).

To confirm the augmentation of Ank^{GAG}1D4-S45Y affinity towards the CA, the CA-binding kinetics of the Ank^{GAG}1D4-S45Y mutant was evaluated by bio-layer interferometry using the BLItz™ system. The kinetic analysis showed that the equilibrium dissociation constant of the binding reaction between CA and Ank^{GAG}1D4-S45Y was found to be $K_D \approx 45$ nM. Ank^{GAG}1D4-S45Y mutant therefore exhibited a significantly higher binding affinity towards the CA, compared to parental Ank^{GAG}1D4 (2.4-fold; **Figure 4**). The kinetic parameters could not be determined for the Ank^{GAG}1D4-Y56A mutant due to the absence of detectable interaction corresponding to **Figure 1A**. Of note, Ank^{GAG}1D4 and Ank^{GAG}1D4-S45Y were both unable to bind recombinant interferon-γ (IFN-γ) which was the irrelevant protein served as negative control (data not shown). This result demonstrated that the S-to-Y mutation at position 45 established a new variant of Ank^{GAG}1D4 which had a superior binding activity towards the HIV-1 CA protein with no change the target specificity, compared to parental Ank^{GAG}1D4.

Viral CA binding site recognition by the Ank^{GAG}1D4-S45Y mutant

The S-to-Y mutation at position 45 in Ank^{GAG}1D4-S45Y might affect the recognition of its CA binding site (referred to as ankyrinotope),[15] and result in the binding of this mutant to a region of the CA different from the initial binding site of the parental Ank^{GAG}1D4. The nature of ankyrinotope(s) of parental Ank^{GAG}1D4 and Ank^{GAG}1D4-S45Y mutant was determined by competitive AMELIA. In the case of Ank^{GAG}1D4-coated conditions, the result showed that both Ank^{GAG}1D4-S45Y mutant and parental Ank^{GAG}1D4 used as competitors significantly diminished the binding activity of Ank^{GAG}1D4 towards the CA protein (**Figure 5**). Interestingly, the ability of Ank^{GAG}1D4-S45Y to compete with Ank^{GAG}1D4 for CA

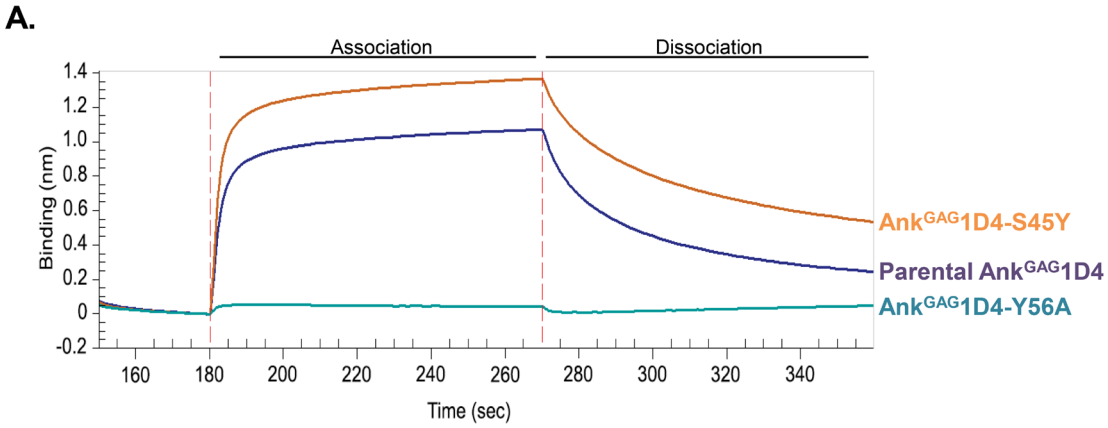

B.

Variants	$k_{on} \times 10^4$ (1/Ms)	$k_{off} \times 10^{-3}$ (1/s)	K_D (nM)
Parental Ank^{GAG}1D4	30.5 ± 5.1	32.8 ± 1.3	109.2 ± 14.9
Ank^{GAG}1D4 -S45Y	40.7 ± 4.1	18.5 ± 0.6	45.6 ± 3.1
Ank^{GAG}1D4 -Y56A	BDL	BDL	BDL

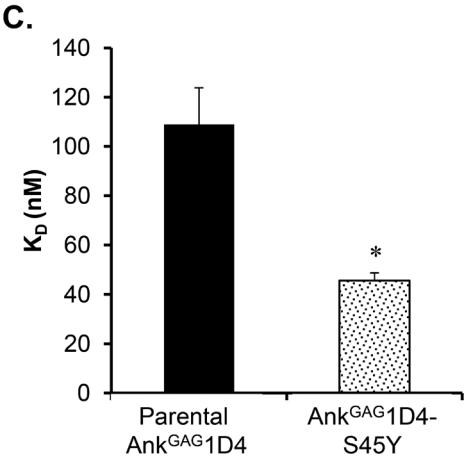

Figure 4. Comparison of CA-binding kinetics of parental Ank^{GAG}1D4 and Ank^{GAG}1D4-S45Y mutant. Binding kinetics were performed using the BLItz™ system. Biotinylated CA protein was immobilized on streptavidin-biosensors and subsequently reacted with recombinant Ank^{GAG}1D4 or Ank^{GAG}1D4-S45Y at 10 µg/mL. (A) Representative sensorgrams displaying the kinetics of the association and dissociation of parental Ank^{GAG}1D4, Ank^{GAG}1D4-S45Y and Ank^{GAG}1D4 Y56A mutants towards biotinylated CA protein. Binding curves were locally fit to a 1:1 binding model and analyzed by the BLItz™ Pro 1.1 software. (B) Kinetic parameters of the binding of Ank^{GAG}1D4-S45Y to the CA protein. BDL indicates that the signals obtained were below detection limit. (C), Comparison the equilibrium dissociation constant values (K_D) of parental Ank^{GAG}1D4 and Ank^{GAG}1D4-S45Y, presented as mean ± SD. Data were analyzed using the Student's t test (*$P < 0.05$).

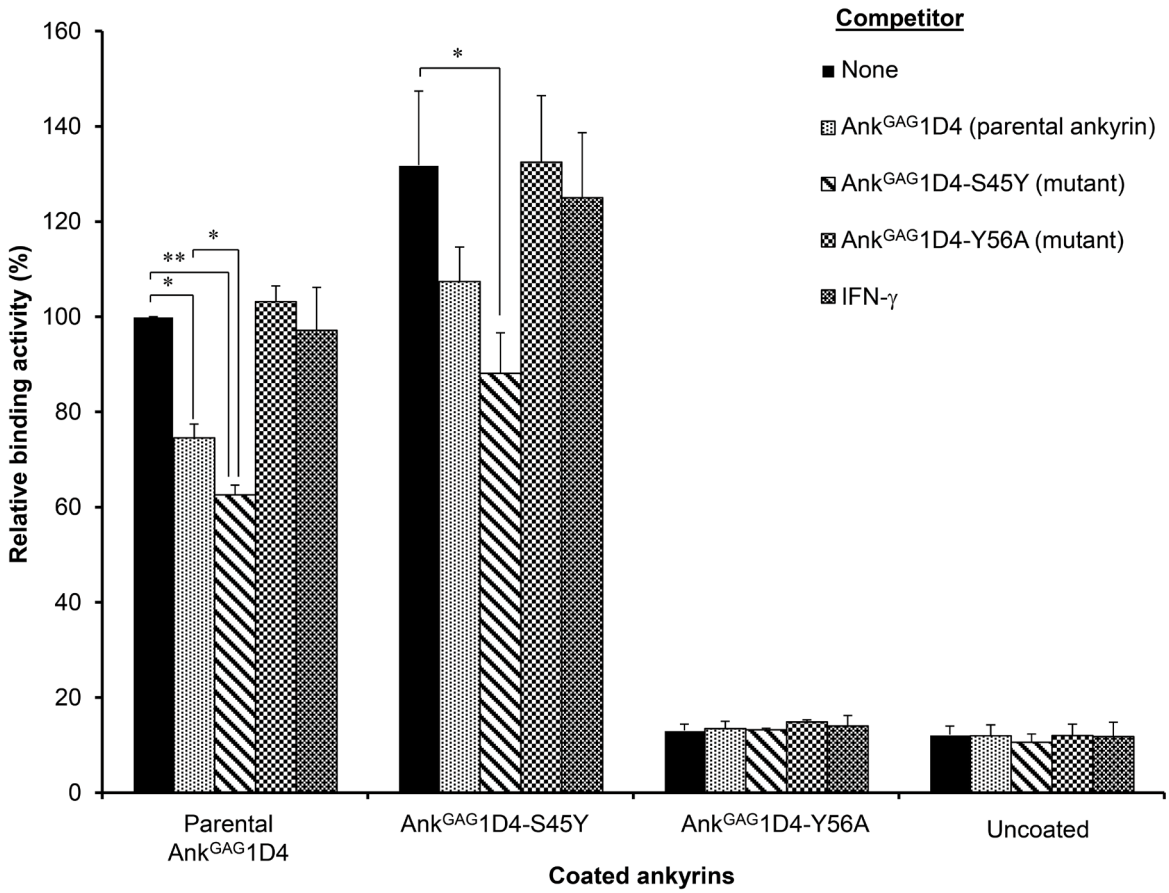

Figure 5. CA ankyrinotope in parental Ank^{GAG}1D4 and Ank^{GAG}1D4-S45Y mutant determined by competitive AMELIA. Immobilized Ank^{GAG}1D4, Ank^{GAG}1D4-S45Y or Ank^{GAG}1D4-Y56A were reacted with biotinylated CA. After removal of the unbound CA, parental or mutant ankyrins were added as competitors for ankyrin-bound CA. Non-binder IFN-γ protein was used as negative control. Ankyrin-bound, biotinylated CA on the solid phase was detected using anti-biotin-HRP. The signal obtained with parental Ank^{GAG}1D4-bound CA in the absence of competitor was attributed the 100% value. The relative binding activity was calculated by the following formula: [$OD_{\text{parental w/ competitors}}$ or $OD_{\text{mutant w/ or w/o competitors}}$/$OD_{\text{parental w/o competitor}}$]×100. All washing steps were performed using high stringency buffer. Results presented are from triplicate experiments (mean ± SD). Data were analyzed using one-way ANOVA. *$P < 0.05$, **$P < 0.01$.

binding was significantly higher than that of the homologous competition of Ank^{GAG}1D4 with itself. No decrease in the binding signal was observed in competition assays with IFN-γ used as the negative control. In the case of Ank^{GAG}1D4-S45Y mutant-coated conditions, only the homologous competition of Ank^{GAG}1D4-S45Y with itself significantly decreased the CA binding activity. Taken together, our results indicated (i) that the Ank^{GAG}1D4-S45Y mutant and parental Ank^{GAG}1D4 recognized the same ankyrinotope on the CA protein, and (ii) that Ank^{GAG}1D4-S45Y mutant bound to the CA with a significantly higher affinity compared to parental Ank^{GAG}1D4.

Discussion

The effectiveness of protein scaffolds essentially depends on their affinity for their targets. The affinity of ankyrins can be enhanced by using various methods, including molecular design, to obtain picomolar range values for the affinity constant.[9] Several reports have described successful improvement of the binding affinity of interacting proteins using computationally guided molecular design.[20-24] Computational design is perfectly adapted to this particular goal, since individual amino acid residue(s), or limited protein domain(s), could be targeted and re-designed while maintaining the folding and three -dimensional structure of the whole molecule and its biological properties.[25]

As applied to our antiviral scaffold Ank^{GAG}1D4, a binder of the HIV-1 CA protein,[13,14] the logical start-point of our affinity enhancement strategy was the modification of amino acid residues which were crucial determinants of the interaction of Ank^{GAG}1D4 with the CA protein. These key residues are the main contributors to the binding energy,[20] and were previously identified in the Ank^{GAG}1D4 molecule docked to its CA target.[15] Tyrosine at position 56 (Y56), the first-rank key residue of the binding surface of Ank^{GAG}1D4,[15] was the first and privileged candidate for site-directed mutagenesis. However, the Y-to-A mutation at position 56 totally abolished the binding activity to the CA target. This result suggested that the first-rank key residue(s) responsible for the ankyrin-target stable interaction was untouchable, and that any type of substitution at such key position(s) would be detrimental to the binding reaction of

ankyrin with its partner. This might be considered as a general guideline for future ankyrin re-engineering.

As a corollary, modifications of second-rank key residues seemed to be the best option to enhance the binding affinity of a given ankyrin to its specific target. S45, R89, K122 and K123 belonged to this class of second-rank key residues of the CA-Ank^{GAG}1D4 interaction.[15] For all positions defined as second-rank key residues, computational predictions revealed that S45Y substitution might confer a significant advantage over the parental Ank^{GAG}1D4 in terms of affinity towards the CA. This was experimentally confirmed using the recombinant mutant Ank^{GAG}1D4-S45Y. The equilibrium dissociation constant of the CA-Ank^{GAG}1D4-S45Y binding reaction was found to be in the nanomolar range of values (K_D = 45 nM), i.e. 2.4-fold lower than with parental Ank^{GAG}1D4. Although modest, this augmentation of affinity was significant and would likely lead to net changes in their biological activities.[26-28] Several studies have shown that combined mutations, and not a single one, are necessary to obtain important increases in the affinity between protein partners.[23,29] Mutation(s) of additional key residues in the Ank^{GAG}1D4-S45Y mutant backbone are therefore envisaged to further enhance the affinity of the Ank^{GAG}1D4-S45Y mutant for its HIV-1 target. These mutations should definitely respect the integrity of the site where the first-rank key residue Y56 resides.

The structural model of HIV-1 CA used in our previous and present studies was the monomeric form of crystallized CA_W184/M185A protein (PDB code: 2LF4), consisting of two independently folded domains, the N-terminal (CA^{NTD}) and C-terminal CA (CA^{CTD}) domains, joined by a flexible linker (YSPTS). Due to this linker, the CA monomer can occur under several isoforms. The three CA isoforms that we have previously chosen among the 20 possible different structures for our simulation of CA-Ank^{GAG}1D4 docking complexes provided an adequate representation of all CA-Ank^{GAG}1D4 complex candidates, and our results suggested that the parental Ank^{GAG}1D4 ankyrin was able to interact with any isoform of HIV-1 CA.[15] Our present results suggested that the S-to-Y mutation at position 45 did not alter the specificity of binding of the Ank^{GAG}1D4-S45Y mutant to the CA as the superimposition between Ank^{GAG}1D4-S45Y (PDB ID 5GIK) and parental Ank^{GAG}1D4 (PDB ID 4HLL) showed 0.16 Å, and that both mutant and parental Ank^{GAG}1D4 recognized the same binding site on the CA protein, located in helix 1 and/or 7 of CA^{NTD}, as previously determined.[15]

In conclusion, we delineated the way to enhance the binding affinity of ankyrin scaffolds to their targets *via* computational design. This new strategy integrated *in silico* predictions through manipulation of key residues combined with vdW binding energy calculation, protein engineering technology and biophysical principle based on bio-layer interferometry analysis. This cross-disciplinary approach opened the way to further modifications and improvement of the binding affinity of next generation ankyrin scaffolds for therapeutic uses in the future. With respect to anti-HIV-1 biotherapy, modified antiviral ankyrins could be introduced into T-cells by episomal or lentiviral vectors in order to generate ankyrin-expressing, HIV-1-resistant cells, as described in our previous studies.[13,14] To validate our concept, such antiviral ankyrins will be applied to hematopoietic stem cells for future clinical applications.[30]

Acknowledgements

The work in Thailand was supported by the National Research Council of Thailand (NRCT), the Cluster and Program Management Office (CPMO), the National Science and Technology Development Agency (NSTDA), the Health Systems Research Institute (HSRI), the National Research University project under the Thailand's Office of the Commission on Higher Education, and the Thailand Research Fund through the Royal Golden Jubilee Ph.D. program (grant number PHD/0146/2556 to K.C. and PHD/0184/2557 to S.M.). The work in Malaysia was supported by the Fundamental Research Grant Scheme (FRGS; grant number FP007-2015A). We are grateful to thank Professor Dr. Watchara Kasinrerk for kindly providing monoclonal antibody against HIV-1 capsid protein. The authors would like to thank the Biomedical Technology Research Center, Faculty of Associated Medical Sciences, Chiang Mai University for giving them access to the BLItz™ system, and also thank Loei Hendrick for his valuable advice in the analysis of BLItz™ results.

Conflict of Interests

The authors declare that they have no conflict of interest.

References

1. Nelson AL, Dhimolea E, Reichert JM. Development trends for human monoclonal antibody therapeutics. Nat Rev Drug Discov. 2010;9:767-74.
2. Reichert JM. Antibodies to watch in 2014. MAbs. 2014;6:5-14.
3. Vaughan AT, Cragg MS, Beers SA. Antibody modulation: limiting the efficacy of therapeutic antibodies. Pharmacol Res. 2015;99:269-75.
4. Chames P, Van Regenmortel M, Weiss E, Baty D. Therapeutic antibodies: successes, limitations and hopes for the future. Br J Pharmacol. 2009;157:220-33.
5. Gilbreth RN, Koide S. Structural insights for engineering binding proteins based on non-antibody scaffolds. Curr Opin Struct Biol. 2012;22:413-20.
6. Jost C, Pluckthun A. Engineered proteins with desired specificity: DARPins, other alternative scaffolds and bispecific IgGs. Curr Opin Struct Biol. 2014;27:102-12.
7. Binz HK, Amstutz P, Kohl A, Stumpp MT, Briand C, Forrer P, et al. High -affinity binders selected from designed ankyrin repeat protein libraries. Nat Biotechnol. 2004;22:575-82.
8. Schweizer A, Roschitzki-Voser H, Amstutz P, Briand C, Gulotti-Georgieva M, Prenosil E, et al. Inhibition of caspase-2 by a designed ankyrin repeat protein: specificity, structure, and inhibition mechanism. Structure. 2007;15:625-36.
9. Zahnd C, Wyler E, Schwenk JM, Steiner D, Lawrence MC, McKern NM, et al. A designed ankyrin repeat protein evolved to picomolar affinity to Her2. J Mol Biol. 2007;369:1015-28.
10. Amstutz P, Binz HK, Parizek P, Stumpp MT, Kohl A, Grutter MG, et al. Intracellular kinase inhibitors selected from combinatorial libraries of designed ankyrin repeat proteins. J Biol Chem. 2005;280:24715-22.
11. Schweizer A, Rusert P, Berlinger L, Ruprecht CR, Mann A, Corthesy S, et al. CD4-specific designed ankyrin repeat proteins are novel potent HIV entry inhibitors with unique characteristics. PLoS Pathog. 2008;4:e1000109.
12. Mann A, Friedrich N, Krarup A, Weber J, Stiegeler E, Dreier B, et al. Conformation-dependent recognition of HIV gp120 by designed ankyrin repeat proteins provides access to novel HIV entry inhibitors. J Virol. 2013;87:5868-81.
13. Nangola S, Urvoas A, Valerio-Lepiniec M, Khamaikawin W, Sakkhachornphop S, Hong SS, et al. Antiviral activity of recombinant ankyrin targeted to the capsid domain of HIV-1 Gag polyprotein. Retrovirology. 2012;9:17.

14. Khamaikawin W, Saoin S, Nangola S, Chupradit K, Sakkhachornphop S, Hadpech S, et al. Combined antiviral therapy using designed molecular scaffolds targeting two distinct viral functions, HIV-1 genome integration and capsid assembly. Mol Ther Nucleic Acids. 2015;4:e249.
15. Praditwongwan W, Chuankhayan P, Saoin S, Wisitponchai T, Lee VS, Nangola S, et al. Crystal structure of an antiviral ankyrin targeting the HIV-1 capsid and molecular modeling of the ankyrin-capsid complex. J Comput Aided Mol Des. 2014;28:869-84.
16. Parks TD, Leuther KK, Howard ED, Johnston SA, Dougherty WG. Release of proteins and peptides from fusion proteins using a recombinant plant virus proteinase. Anal Biochem. 1994;216:413-7.
17. Ashkenazy H, Abadi S, Martz E, Chay O, Mayrose I, Pupko T, et al. ConSurf 2016: an improved methodology to estimate and visualize evolutionary conservation in macromolecules. Nucleic Acids Res. 2016;44:W344-50.
18. Suzek BE, Wang Y, Huang H, McGarvey PB, Wu CH. UniRef clusters: a comprehensive and scalable alternative for improving sequence similarity searches. Bioinformatics. 2015;31:926-32.
19. Kyte J, Doolittle RF. A simple method for displaying the hydropathic character of a protein. J Mol Biol. 1982;157:105-32.
20. Reichmann D, Rahat O, Cohen M, Neuvirth H, Schreiber G. The molecular architecture of protein-protein binding sites. Curr Opin Struct Biol. 2007;17:67-76.
21. Nisius B, Sha F, Gohlke H. Structure-based computational analysis of protein binding sites for function and druggability prediction. J Biotechnol. 2012;159:123-34.
22. Mikulecky P, Cerny J, Biedermannova L, Petrokova H, Kuchar M, Vondrasek J, et al. Increasing affinity of interferon-gamma receptor 1 to interferon-gamma by computer-aided design. Biomed Res Int. 2013;2013:752514.
23. Lippow SM, Wittrup KD, Tidor B. Computational design of antibody -affinity improvement beyond in vivo maturation. Nat Biotechnol. 2007;25:1171-6.
24. Tue-ngeun P, Kodchakorn K, Nimmanpipug P, Lawan N, Nangola S, Tayapiwatana C, et al. Improved scFv anti-HIV-1 p17 binding affinity guided from the theoretical calculation of pairwise decomposition energies and computational alanine scanning. Biomed Res Int. 2013;2013:713585.
25. Erijman A, Rosenthal E, Shifman JM. How structure defines affinity in protein-protein interactions. PLoS One. 2014;9:e110085.
26. Martin F, Toniatti C, Salvati AL, Ciliberto G, Cortese R, Sollazzo M. Coupling protein design and in vitro selection strategies: improving specificity and affinity of a designed beta-protein IL-6 antagonist. J Mol Biol. 1996;255:86-97.
27. Chang J, Jin J, Lollar P, Bode W, Brandstetter H, Hamaguchi N, et al. Changing residue 338 in human factor IX from arginine to alanine causes an increase in catalytic activity. J Biol Chem. 1998;273:12089-94.
28. Walensky LD, Kung AL, Escher I, Malia TJ, Barbuto S, Wright RD, et al. Activation of apoptosis in vivo by a hydrocarbon-stapled BH3 helix. Science. 2004;305:1466-70.
29. Lippow SM, Tidor B. Progress in computational protein design. Curr Opin Biotechnol. 2007;18:305-11.
30. Kiem HP, Jerome KR, Deeks SG, McCune JM. Hematopoietic -stem-cell-based gene therapy for HIV disease. Cell Stem Cell. 2012;10: 137-47.